




Original Article

Application of an unsupervised clustering algorithm on *in situ* broadband acoustic data to identify different mesopelagic target types

Mette Dalgaard Agersted ^{1,*}, Babak Khodabandloo², Yi Liu², Webjørn Melle¹, and Thor A. Klevjer¹

¹Plankton Research Group, Institute of Marine Research, P.O. Box 1870, Nordnes, NO-5817 Bergen, Norway

²Ecosystem Acoustics Research Group, Institute of Marine Research, P.O. Box 1870, Nordnes, NO-5817 Bergen, Norway

*Corresponding author: tel: +4521812063; e-mail: mette.dalgaard.agersted@hi.no

Agersted, M. D., Khodabandloo, B., Liu, Y., Melle, W., and Klevjer, T. A. Application of an unsupervised clustering algorithm on *in situ* broadband acoustic data to identify different mesopelagic target types. – ICES Journal of Marine Science, 78: 2907–2921.

Received 9 April 2021; revised 29 July 2021; accepted 2 August 2021; advance access publication 31 August 2021.

The mesopelagic zone (200–1000 m depth) contains high fish species diversity but biomass and abundances are uncertain yet essential to understand ecosystem functioning. Hull-mounted acoustic systems (usually 38 kHz) often make assumptions on average target strength (TS) of mesopelagic fish assemblages when estimating biomass/abundance. Here, an unsupervised clustering algorithm was applied on broadband acoustic data (54–78 kHz), collected by a towed instrumented platform in the central Northeast Atlantic, to identify different mesopelagic target types based on similarity of individual TS spectra. Numerical density estimates from echo-counting showed spatial differences in vertical distribution patterns of the different target types and TS spectra data suggested that >30% of the gas-bearing targets had high resonance frequencies (>60 kHz) with low scattering strength at 38 kHz. This conceptual study highlights the importance of separating targets into different target groups to obtain correct backscatter information and to account for all relevant scatterers when estimating average TS at 38 kHz, in order to achieve more accurate biomass/abundance estimates. It furthermore demonstrates the use of a towed broadband acoustic platform for fine-scale numerical density estimates as a complementary method to hull-mounted acoustic data to increase knowledge on mesopelagic ecosystem structure.

Keywords: agglomerative clustering, hull-mounted acoustics, target strength spectra, towed acoustic platform, viscous–elastic scattering model

Introduction

The mesopelagic zone ranging from 200 to 1000 m depth potentially possesses high abundance and biomass of fish (Gjøsæter and Kawaguchi, 1980; Irigoien *et al.*, 2014; Davison *et al.*, 2015; Proud *et al.*, 2019) and also crustaceans, squids, and jellyfish are present. A proportion of the mesopelagic fauna performs diel vertical migration (DVM) (Gjøsæter and Kawaguchi, 1980; Klevjer *et al.*, 2016), feeding in the euphotic zone during night while descending to deeper depths at dawn to hide from visual predators (Hays, 2003). This behaviour leads to active transport of carbon from upper

waters to the deep ocean (e.g. Robinson *et al.*, 2010; Davison *et al.*, 2013), contributing to carbon sequestering. Mesopelagic organisms have mostly been studied throughout the oceans in the context of the so-called deep scattering layers (DSLs), i.e. layers that are identified by their ability to scatter sound. The vertical distribution of these DSLs varies geographically and can range from tens to hundreds of metres vertically and can continue for tens to thousands of kilometres horizontally (Irigoien *et al.*, 2014; Klevjer *et al.*, 2016, 2019). The vertical position of DSLs has been linked to various environmental parameters such as oxygen concentration (Bianchi *et al.*, 2013; Klevjer *et al.*, 2016) and light intensity

(Aksnes *et al.*, 2017). Furthermore, there can be more than one DSL within the mesopelagic zone, most likely constituted by different species and/or types or sizes of organisms (e.g. Andreeva *et al.*, 2000; Dypvik *et al.*, 2012; Ariza *et al.*, 2016). When DSLs are identified from acoustic data obtained with low-frequency (i.e. 18 and 38 kHz), hull-mounted transducers, the identification and delineation of these DSLs are inherently biased towards layers containing organisms with gas inclusions (Klevjer *et al.*, 2012; Underwood *et al.*, 2020), since these organisms tend to give stronger echoes at low frequencies.

Acoustic techniques are non-extractive, and hull-mounted narrowband acoustic systems are often used in both epipelagic and mesopelagic studies to measure backscattering from fish and other organisms as a proxy for abundance and/or biomass (Simmonds and MacLennan, 2005). One limitation of sound transmitted from surface waters is that it is generally not possible to isolate the backscatter from individual organisms in deep waters, as the volume of the acoustic beam increases with depth (Simmonds and MacLennan, 2005) (a transducer with an opening angle of 7° will have a beam diameter of ~61 m at 500 m, a typical depth of DSLs), and as the backscatter originates from an assemblage of organisms, each of which may have very different acoustic properties. Another limitation is absorption by water (Francois and Garrison, 1982a, 1982b), which limits the working range of higher frequencies (i.e. >~100 kHz; for the echosounders that we have used, a frequency of 120 kHz with the transmit power of 250 W will have a working range of ~300 m, though dependent on noise from e.g. rain and wind-induced waves (Furusawa, 2015)) (Simmonds and MacLennan, 2005). While this is not a problem when studying the epipelagic zone, only lower frequencies (typically 18 and 38 kHz) can reach the deep part of the mesopelagic zone from the surface. The absorption issue can be avoided by applying towed platforms equipped with acoustic instruments to obtain high-frequency acoustic measurements of individual mesopelagic organisms also in deep waters (e.g. Kloser *et al.*, 2016; Bassett *et al.*, 2020). This approach will furthermore increase the possibility of getting backscatter measurements of single targets inside the acoustic beam.

Target strength (TS), i.e. the logarithmic measure of the proportion of acoustic energy that a single target backscatters to the acoustic source (Simmonds and MacLennan, 2005), depends on an organism's material properties (density and sound speeds), size, shape, and orientation in relation to the incoming sound pulse (Faran Jr, 1951; Hickling, 1962; Stanton *et al.*, 1998). For organisms with a gas inclusion (like swimbladder fish or physonect siphonophores), the gas bladder is the main reflector and usually accounts for more than 90% of the total backscattered energy (Foote, 1980). Information on organisms' TSs is crucial, as the total backscattering energy from aggregations of organisms, together with the mean TS of the assemblage, are used to estimate abundance (Simmonds and MacLennan, 2005). Of particular importance in the use of acoustics to estimate the abundance of mesopelagic fish is the influence of acoustic resonance. For a "resonant" organism, TS peaks at the resonant frequency, resulting in a TS significantly higher than that for a non-resonant organism. Yet, TS changes very rapidly close to the resonance frequency, which in practice makes it difficult to assign TS values to "resonant" organisms, since very small changes in size of gas inclusion, pressure (i.e. depth), and material properties can give rise to very large changes in TS (e.g. Kloser *et al.*, 2016; Proud *et al.*, 2019). Swimbladder resonance could further cause bias in biomass/abundance estimates as

small swimbladder fish could cause an increase in backscatter. On top of this, acoustically weaker targets may be overlooked due to the strong backscattering from "resonant" organisms, thus further leading to wrong estimates of actual abundance and biomass of mesopelagic communities (Underwood *et al.*, 2020). Newer studies estimate average TSs by different approaches using literature values (e.g. Irigoien *et al.*, 2014) or trawl catches in connection with acoustic backscattering models (e.g. Davison *et al.*, 2015; Proud *et al.*, 2019). As catches from mesopelagic depths rarely consist of a single species or type of organism (Ariza *et al.*, 2016; García-Seoane *et al.*, 2021), separating backscatter information into different types of organisms (i.e. "target types") and obtaining TSs for these different groups would increase the possibility of obtaining more accurate abundance and biomass estimations of mesopelagic communities.

Multifrequency acoustics are frequently used to distinguish between major scattering groups based on their relative frequency response at discrete frequencies (Korneliussen and Ona, 2002; Korneliussen *et al.*, 2016). The obtained frequency response information is usually not adequately detailed to separate acoustically similar species or different size groups of a single species (De Robertis *et al.*, 2010). In comparison, broadband acoustics can provide high-resolution frequency response data (i.e. "acoustic fingerprints"), which potentially can be used for identification and separation of different organismal types and to identify regions where resonance occurs (e.g. Horne, 2000; Stanton *et al.*, 2010; Bassett *et al.*, 2018, 2020). Combined with scattering models, the measured broadband frequency response data can further be used to explore physical characteristics of the organism (e.g. body flesh density and swimbladder radius; Khodabandeloo *et al.*, 2021). Furthermore, the higher range resolution (compared to narrowband acoustic systems) obtained through matched filtering (Lavery *et al.*, 2009; Stanton *et al.*, 2010) can enable separation of single targets at close ranges when targets are not too dense inside the acoustic beam. Resolving single targets/echoes makes it possible to estimate numerical densities through echo-counting (e.g. Simmonds and MacLennan, 2005; Kloser *et al.*, 2016; Cotter *et al.*, 2021b) as a supplement to hull-mounted acoustic abundance estimates. The increased backscattering information obtained from broadband acoustic systems can eventually be used to study behaviour and distribution patterns of different target/organismal types *in situ*, e.g. along spatial gradients, thereby adding to our limited knowledge on mesopelagic ecosystems.

Identifying single broadband acoustic targets manually is, however, very time-consuming and furthermore not objective. Unsupervised clustering algorithms, where data are grouped according to similarity (e.g. Peña, 2018), could be an alternative approach in identifying patterns in big data, like broadband acoustic data, and being particularly beneficial for data interpretation when, for example, net data, for ground-truthing of the acoustic measurements, are not available.

The focus of this paper is to demonstrate the application of an unsupervised machine learning algorithm (clustering) on *in situ* measured broadband TS spectra from gas-bearing mesopelagic organisms obtained from a towed platform at depths ranging from surface to 1000 m. Different acoustic target types were identified based on similarities of TS spectra and a viscous-elastic scattering model applied to estimate resonance frequency of the different target types. The vertical distribution of organisms with different acoustic properties has implications for interpretations of acoustic data from hull-mounted transducers, so we additionally evaluate the influence of vertical distribution on abundance estimates from

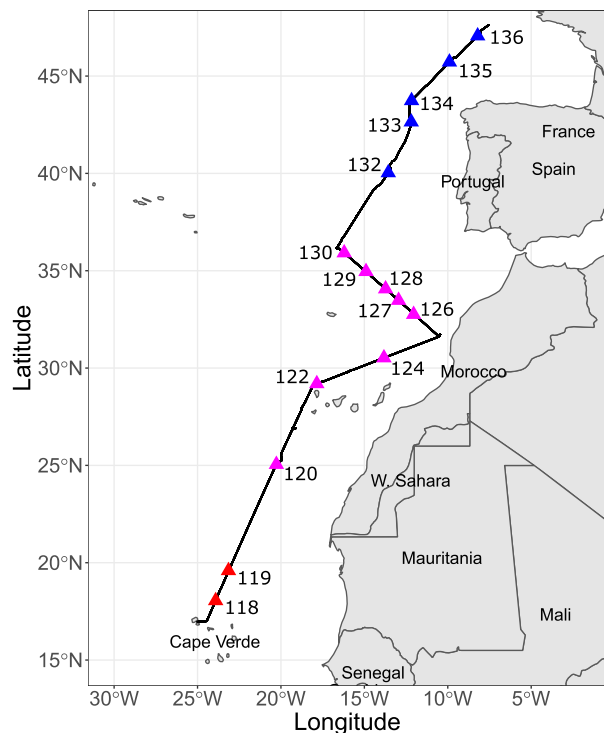


Figure 1. Map of cruise track (black line) and stations where MESSOR collected acoustical data (southern region: red triangles, $n = 2$; central region: magenta triangles, $n = 8$; and northern region: blue triangles, $n = 5$).

hull-mounted systems. We furthermore present the applicability of this approach in combination with echo-counting to obtain estimates on numerical densities and distribution patterns of organisms in the mesopelagic zone as a supplement to hull-mounted acoustic data. This information can add to our understanding of spatial structures of mesopelagic communities, and ultimately be used to investigate which acoustic groups of mesopelagic organisms that perform DVM and to study organismal-facilitated active carbon transport. Furthermore, this enables us to better understand the relative importance of resonance in measurements of acoustic backscattering intensity at different frequencies, and to estimate abundance and biomass of mixed assemblages, which may lead to robust interpretations of patterns in hull-mounted acoustic data.

Material and methods

Data used in this paper were collected during a research cruise in the eastern part of the Mid-Atlantic Ocean from Cape Verde to Bay of Biscay (17°N 25°W to 48°N 8°W) (Figure 1) onboard R/V Kronprins Haakon (Norwegian Institute of Marine Research) from 2 to 22 May 2019. The objective was to advance our understanding of the mesopelagic ecosystem along latitudinal and longitudinal gradients in the studied area.

Acoustic measurements

Acoustic data collected by towed platform

At each station ($n = 15$) marked in Figure 1, a towed acoustic platform (MESSOR; Knutsen *et al.*, 2013) was deployed to

measure backscattering intensity from organisms throughout the mesopelagic zone. MESSOR was equipped with a four channel echosounder [Simrad EK80 WBT Tubes operating at nominal frequencies of 38 (narrowband, broadband mode was not an option) and 70, 120, and 200 kHz (broadband)], but only data from 70 kHz (50–80 kHz) were used here. The transducers were mounted on the bottom plate of MESSOR, facing downwards. See Supplementary Table S1 for data collection settings and Khodabandeloo *et al.* (2021) for further details, including calibration of MESSOR. A CTD (Seabird SBE 49 FastCAT) mounted on MESSOR was operated throughout the deployments and used to estimate density and sound speed of the surrounding seawater as a function of depth.

MESSOR was towed behind the ship obliquely from 0 to 1000 m depth with a speed of 4 knots, measuring both during descend and ascend. At most stations, MESSOR was deployed to cover the transition from night to daytime. To separate day from night data, the sun angle (altitude) was calculated for each measurement by using information on position (date, time, latitude, and longitude) by using the package “oce” in R statistical software (R Core Team, 2018; Kelley and Richards, 2020). Day and night were defined as sun angle being $> 0^\circ$ and $< 0^\circ$ relative to the horizon (i.e. altitude), respectively. We only obtained both night and daytime measurements throughout the mesopelagic zone at three stations, and the remaining stations did not have both a complete day and night vertical profile.

Hull-mounted acoustic data

Narrowband acoustic data were collected at 18, 38, and 70 kHz by the vessel’s hull-mounted Simrad EK80 echosounder system both at stations and along the cruise transect (at a vessel speed of 10 nmi). Calibration of the system was conducted using standard methods (Demer *et al.*, 2015) with a 38.1-mm-diameter tungsten carbide (with 6% cobalt binder) sphere. See Supplementary Table S2 for settings and calibration parameters. Spike noise from the acoustic Doppler current profiler on the trawl and Scanmar on the Multinet (which both were deployed at each station), were removed by applying noise filters using the software LSSS, version 2.8.0 (Large Scale Survey System, Korneliussen *et al.*, 2016). Noise from false bottom and surface bubbles were removed by manual scrutiny in LSSS. Backscattering data were afterwards integrated in 5-meter vertical by 10 minutes horizontal bins at a mean volume backscattering strength (S_v , dB *re* 1 m^{-1}) threshold of -85 dB *re* 1 m^{-1} . After integration, the backscatter data were corrected for errors caused by the nominal sound-absorption coefficient and sound-speeds used in LSSS (LSSS permits only a single, static value for sound-absorption) following Haris *et al.* (2021). These corrections were based on dynamic, vertical profiles of sound-speed and absorption (Francois and Garrison, 1982a, 1982b) calculated from vertical profiles of temperatures and salinities recorded at the stations by a SBE 911 plus CTD (Sea-Bird Electronics, WA, USA), with values interpolated between stations.

For each MESSOR deployment, we created a corresponding vertical profile of backscatter from the hull-mounted echosounders. As MESSOR was towed behind the vessel, it would have been about 11 min behind the vessel when MESSOR was at its deepest (1000 m). Hence, the data from MESSOR and the hull-mounted acoustic system were not exactly concurrent, and the spatial/temporal mismatch was dealt with by averaging the integrated hull-mounted data recorded within 10 m vertical and 1 hour of the time/depth coordinate observed from MESSOR.

Table 1. Settings used to automatically detect single targets using the acoustic analytical software LSSS.

Target detector settings	
Minimum TS (dB)	−70
Pulse length determination level (dB)	20
Minimum echo length (relative to pulse length)	0
Maximum echo length (relative to pulse length)	1
Max (one way) gain compensation (dB)	3
Frequency resolution (kHz)	1

Automatic target extent window for fast Fourier transformation was used as spectrum extraction setting.

Analysing acoustic data from MESSOR

Acoustic data obtained from MESSOR (15 deployments, Figure 1) were analysed using LSSS. Data from the echosounder channel with the nominal frequency of 70 kHz (50–80 kHz) were processed to yield *in situ* measurements of TS as a function of frequency [TS(f); henceforth “TS spectra”] of mesopelagic organisms. This frequency range was chosen as this was the lowest frequency band where broadband measurements were available. We automated the target detection by applying a single echo detection algorithm (Ona, 1999) in LSSS (for detection settings, see Table 1). Echoes that had a weaker TS in the 54–78 kHz band were rejected to remove echoes from weaker scatterers such as crustaceans and jellyfish. Inspection of TS histograms of data from the 70 kHz band showed local minima at −68 dB *re* 1 m², which was hence chosen as a TS threshold to separate strong and weaker targets (i.e. at least one TS value within the frequency band must have the value of minimum −68 dB *re* 1 m² to be accepted as a target). The remaining TS spectra were likely from gas-bearing targets and/or large non-swimbladdered fish (e.g. Stanton *et al.*, 2010; Davison, 2011). We did not reject echoes based on phase deviation of samples to lessen the potential impact of rejecting echoes from regions with high densities of targets.

TS values for all individual targets and the TS spectra were exported in 1 kHz frequency resolution and post-processed in RStudio statistical software (R Core Team, 2018). Target data were subsetted to include only data from a range of 9–12 m from MESSOR. This shorter range was chosen to avoid possible avoidance very close to MESSOR, as observed for mesopelagic fish in relation to a profiling acoustic probe (Bernardes *et al.*, 2020), although there could potentially have been avoidance from larger fish at the chosen range. The longer range was chosen to avoid bias in densities caused by overlapping echoes or reduction in detection probabilities of echoes as a consequence of changes in signal-to-noise ratios (e.g. Mulligan, 2000).

Cluster analysis

The absolute TS spectra for all targets, i.e. every single TS measured at each frequency in 1-kHz frequency resolution, were plotted in a histogram to investigate the dataset further. Based on the histogram, it was decided to remove targets where the TS spectra had values that exceeded the ± 0.5 percentiles of the raw data to remove possible noise/outliers. That is, if a target's frequency spectrum had TSs included, which were outside of the minimum and maximum TS values (0.5th and 99.5th percentiles, per “discrete” frequency), the target was excluded from the dataset. The filtered data were used for further analysis ($n = 67192$ targets). We have acoustic

data from both night and day, and hence, some mesopelagic organisms that perform DVM will be present in the upper 200 m during night. Therefore, all detected targets between the surface and 1000 m depth were included in the clustering analysis.

Among many popular clustering techniques (spectral clustering, mean shift, *k*-means, affiliation propagation, Gaussian mixture clustering, DBSCAN, and HDBSCAN, etc.), we use the hierarchical agglomerative clustering (AC) algorithm for its merits of (i) scalability to large datasets, (ii) efficiency with an optimized time complexity of $O(n^2 \log n)$, (where complexity O is the complexity of the algorithm given input size n), and (iii) empirical outperformance over other methods on our experimental data. The AC algorithm starts off by having each observation (n) as a single object/cluster (singleton) and proceeds to merge the most similar clusters until a stopping criterion, such as a decided number of clusters, is met (e.g. Jain *et al.*, 1999; Javed *et al.*, 2018). Empirically, we set Ward's linkage that minimizes the variance of the clusters being merged (Ward, 1963). Here, we applied an elbow algorithm (e.g. Subramaniyan *et al.*, 2020) using 2–30 clusters for a proper number of clusters that measures the compactness of the clustered results. For the clustering and elbow analyses, frequency response [r(f)] data for each target ($n = 67192$) were normalized relative to r(f) at 70 kHz, when TS₇₀ was set to zero and targets were divided into cluster types based on their r(f). Note that this is mathematically an affine mapping operation, which keeps shape and slope of their r(f) unchanged hence highlighting the shape and slope in the clustering process.

Spatial distribution of target types

The vertical and horizontal distributions of the different TS spectra types were investigated throughout the studied area in the mesopelagic zone during day and night. Echo-counting was applied to the clustered data from all 15 MESSOR stations, yielding estimates of *in situ* numerical densities per cluster.

Since the clustered single echo detections were obtained within the 3-dB beam width (i.e. with a one-way beam compensation of less than 3 dB), we estimated organism densities per ping (ρ):

$$\rho = \frac{n_{sed}}{n_{ping} \times V_{obs}}, \quad (1)$$

where n_{sed} is the number of detected single echoes, n_{ping} is the number of transmitted sound pulses, and V_{obs} is the sampled volume, which was estimated as the volume of a cone, based on the nominal transducer 3-dB beam width. The per ping estimates of organism densities were averaged over 30 second intervals to produce datasets of reduced resolution and variability. Density data are shown with 10-m vertical resolution.

Resonance frequency estimates

We only used a relatively narrow frequency range to identify the different cluster types but TS frequency response and level of the selected targets suggest that they were from gas-bearing (i.e. swimbladdered) fish. Thus, to estimate the frequency responses of gas-bearing targets over a wider frequency range to obtain an estimate of resonance frequencies of the different cluster types, we applied the viscous-elastic scattering model presented in Khodabandeloo *et al.* (2021). We did not fit the model to the average TS spectra of all targets of a cluster type, but randomly selected single targets situated within the centroids of each cluster type for the model fitting ($n = 5$ per cluster type) to minimize overlap between target/cluster

types. The model was fitted to the TS spectra measured from 60 to 76 kHz. Due to small swimbladder size and being in deep water, this frequency range is close to the resonance of mesopelagic species (Khodabandloo *et al.*, 2021). The swimbladder accounts for most of the backscattering near the resonance frequency region (Foote, 1980; Feuillade and Nero, 1998). Furthermore, since the resonance region is not significantly sensitive to the swimbladder shape (Feuillade and Nero, 1998; Ye and Hoskinson, 1998), we applied a spherical backscattering model for all the targets to estimate the swimbladder volume. To fit the model around the resonance area (Khodabandloo *et al.*, 2021), swimbladder size [i.e. equivalent spherical radius (ESR)] and flesh viscosity were the two tunable model parameters, and depth of the targets were used to estimate the gas density inside the swimbladder. For details on model parameters and fitting, see Khodabandloo *et al.* (2021). Estimating resonance frequencies enabled us to evaluate the vertical distribution patterns of the different cluster types with that of the backscattering measured by the hull-mounted acoustic data at 18, 38, and 70 kHz.

Results

Cluster analysis

The elbow algorithm resulted in an optimal cluster number of seven (see Supplementary Figure S1), and this number was subsequently used when performing the AC algorithm. The corresponding seven (average) frequency responses for each of the cluster types are displayed in Figure 2. For visualization, the AC result is plotted in a Principal Component Analysis (PCA) space (Supplementary Figure S2).

Some of the cluster types have similar average $r(f)$ spectra, i.e. similar shapes [e.g. decreasing $r(f)$ with increasing frequency] but differed in TS ranges and resonance frequencies (Figure 2 and Table 2). As the TS spectra assigned to each of the seven cluster types all are average TS spectra, there can be large differences between TS spectra within one cluster type, which is also evident in the PCA space where it is apparent that there are some overlap between “neighbouring” cluster types (Supplementary Figure S2).

The dominating cluster/target type from 200 to 1000 m depth throughout the cruise was C6, followed by C1, C0, and C2 (Table 2). The less abundant types, not considering C3, were C4 and C5 targets, which occurred in similar numbers. C3 did not have a clear resonance peak and due to the low contribution (close to 0%) to the total targets in the mesopelagic zone (Figure 2 and Table 2), C3 will not be considered in the following.

Resonance frequency estimations of cluster types

The viscous–elastic scattering model developed by Khodabandloo *et al.* (2021) was applied on *in situ* measured TS spectra of targets ($n = 5$ per cluster) to estimate resonance frequencies for the cluster types (Figure 3). Displayed targets were detected from 302 to 923 m depth and had estimated swimbladder ESR ranging from 0.214 to 0.767 mm.

Based on the fitted model, it is evident that ~30% (C2, C4, and C5) of the randomly chosen targets from all cluster types ($n = 5$ per cluster type) had low TSs at 38 kHz (Figure 3 and Table 2). Of the chosen targets, the cluster types C4 and C5 had resonance within the frequency window, whereas C2 had increasing TS with frequency (Figure 3), i.e. resonance at frequencies >76 kHz.

Together, these clusters (C2, C4, and C5) represent less than 30% of all registered echoes (Table 2). However, also some of the random targets of cluster types C0, C1, and C6 showed estimated resonance frequencies >38 kHz, leading us to estimate that more than 30% of targets had resonant frequencies higher than 38 kHz.

Spatial variation in hull-mounted acoustic backscatter

The vertical distribution of mesopelagic backscatter differed between the three different frequencies (18, 38, and 70 kHz) from the hull-mounted acoustic data (Figure 4). Based on the structure of the mesopelagic backscatter along the transect, three different areas were inferred regarding vertical distribution patterns of DSLs and intensity of backscattering strength: south (stations 118 and 119, south of 20°N), central (stations 120–130, 25–37°N) and north (stations 132–136, north of 40°N).

Vertical distribution of cluster types in the mesopelagic zone

Night-time profiles from MESSOR were available at all but three stations, whereas only five daytime profiles were fully covered. Therefore, comparisons between day- and night-time vertical distribution patterns for single stations are difficult. Accordingly, backscattering data [Nautical Area Scattering Coefficient (NASC; $m^2 \text{ nmi}^{-2}$) from hull-mounted] and numerical density estimates (MESSOR) were merged per instrument for the three different areas mentioned above (south, central, and north), and furthermore separated into day- and night-time profiles (Figures 5–7) for better comparison of hull-mounted and MESSOR data. See e.g. Supplementary Figure S4 for vertical distribution and numerical densities at each station (from MESSOR profiles). Cluster type C3 constituted 0.04% of total densities and are therefore not included in the result section.

The southern region only consists of two MESSOR stations and only a single night profile, which makes it difficult to compare day and night vertical distribution patterns due to some differences in the vertical distribution patterns of targets between st.118 and 119 (see e.g. Supplementary Figure S4). Nonetheless, it is apparent that the densities in the mesopelagic zone are lower during night than day at st.118, where both a day and night profile are available (Supplementary Figure S4, Figure 5a and c). The lower numerical density of targets during night compared to daytime supports DVM as also observed in the hull-mounted data (Figures 4 and 5a and c). During daytime, the two most abundant cluster types, C6 and C1, occurred mainly in two distinct layers corresponding to DSL1 (highest densities of C6) and DSL2 (highest densities of C1) observed in the hull-mounted data (Figures 4 and 5a). C0 targets also had relatively high densities during day and peaked in DSL2, slightly deeper than the peak of C1 targets. C2 targets peaked in DSL1, slightly deeper than the peaks of C1 and C6 targets. C4 peaked in the upper part of DSL2.

Compared to the south, the vertical distribution patterns of targets differed in the central region where one main DSL1 was present. Total numerical densities were very similar during day and night (Figure 6a and c), suggesting little DVM. Overall, C6 targets had highest densities and peaked within the DSL1 (measured at 38 kHz, Figure 4). As opposed to the south, C6 targets occurred slightly deeper than the other target types. Cluster types C0, C1, C2, and C4 had slightly lower integrated densities at night compared to

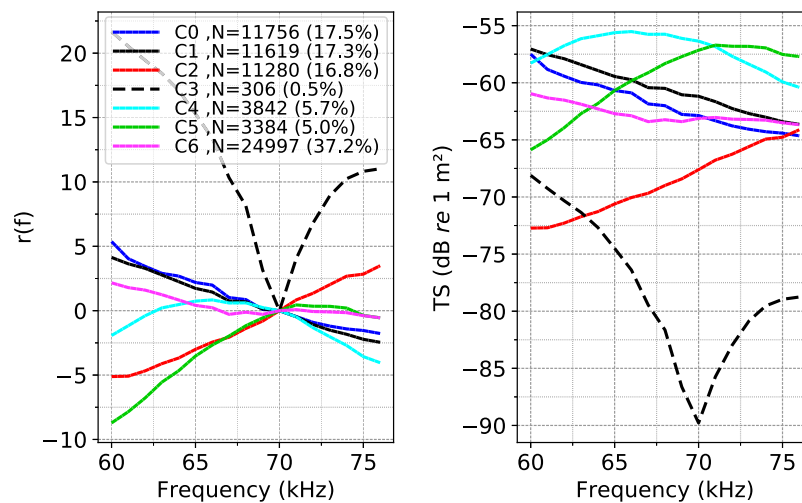


Figure 2. Left graph displays average frequency response $[r(f)]$ spectra of the seven cluster types C0–C6 relative to TS measured at 70 kHz (TS_{70}). Contribution of each cluster type to the total ($n = 67192$) numbers of targets detected from 0 to 1000 m depth is listed. Right graph displays the corresponding TS spectra of cluster types C0–C6. For each identified cluster type, we define the cluster spectrum as the average value per frequency, i.e. for the $r(f)$ spectra (left panel), each line represents the per frequency average $r(f)$ and for the TS spectra (right panel), each line represents the per frequency average TS for each cluster. Note that colours for the different clusters are not corresponding to the colours in Supplementary Figure S2. For the relative contribution and numbers of the cluster types in the mesopelagic zone, see Table 2.

Table 2. Cluster types 0–6 listed from the most to less dominating throughout the cruise from 200 to 1000 m depth.

Cluster/target type	Shape	TS range (dB)	Resonance frequency
C6 ($n = 15\,772$, 34.8%)	Decrease with frequency	–61 to –64	<60 kHz
C1 ($n = 8365$, 18.4%)	Decrease with frequency	–57 to –64	<60 kHz
C0 ($n = 8207$, 18.1%)	Decrease with frequency	–58 to –65	<60 kHz
C2 ($n = 7829$, 17.3%)	Increase with frequency	–64 to –73	>76 kHz
C4 ($n = 2854$, 6.3%)	Peak within window	–56 to –60	Between 60 and 76 kHz
C5 ($n = 2321$, 5.1%)	Peak within window	–57 to –66	Between 60 and 76 kHz
C3 ($n = 16$, 0.04%)	“v”-shaped	–68 to –90	No clear peak

A total of 45364 targets were detected 9–12 m from MESSOR and the numbers detected for each target type are stated in parentheses, together with the relative contribution (%). The shape, TS range (rounded to nearest kHz) and resonance frequencies of the average TS spectra inside the frequency window (60–76 kHz; Figure 2) are reported.

daytime. These cluster types peaked in densities between ~470 and 520 m depth, associated with DSL1 (Figure 4). Lower density peaks were observed ~600–650 m depth.

In the northern region, densities of targets were generally lower (Figure 7a and c) compared to the south and central. Overall, C6 targets dominated with peak densities at similar depth day and night. During day, C6 targets were present in two DSLs (DSL1 and DSL2) but one main layer at night (DSL2). Densities of the other target types were very low and in general similar day and night for all the target types, indicating little DVM as also observed in the hull-mounted data (Figures 4 and 7a and c). The second most abundant target type was C2, which showed increasing densities below ~800 m depth.

Comparing backscatter measured by hull-mounted and towed acoustic systems

Similar for all regions was that distribution patterns of C6 targets seem to correspond with backscattering measured by the hull-mounted 38 kHz, whereas the remaining target types (most evident when for example looking at densities of C0, C1, C2, and C4

targets in the central region), followed the backscatter measured by the hull-mounted echosounder at 70 kHz (Figures 5–7). In general, hull-mounted 18 kHz NASC data did not correlate with high densities or NASC values obtained from MESSOR for any cluster type. For example, during night-time in the southern region and daytime in the northern, backscatter at 18 kHz was substantial from ~200 to 400 m depth, but this was not at all evident in the density estimates from MESSOR (Figures 5d and 7b).

The hull-mounted backscattering data measured at 70 kHz were in overall good agreement with the 70 kHz MESSOR data in the upper 560 m where hull-mounted 70 kHz data were available (see e.g. Figures 5b and 6b and d). The densities estimated from 70 kHz MESSOR data were decoupled from the NASC patterns of the hull-mounted 38 and 18 kHz transducers (Figures 5–7).

Discussion

Target identification

Previous studies have suggested the possibility of applying broad-band acoustic data to separate and identify different organismal

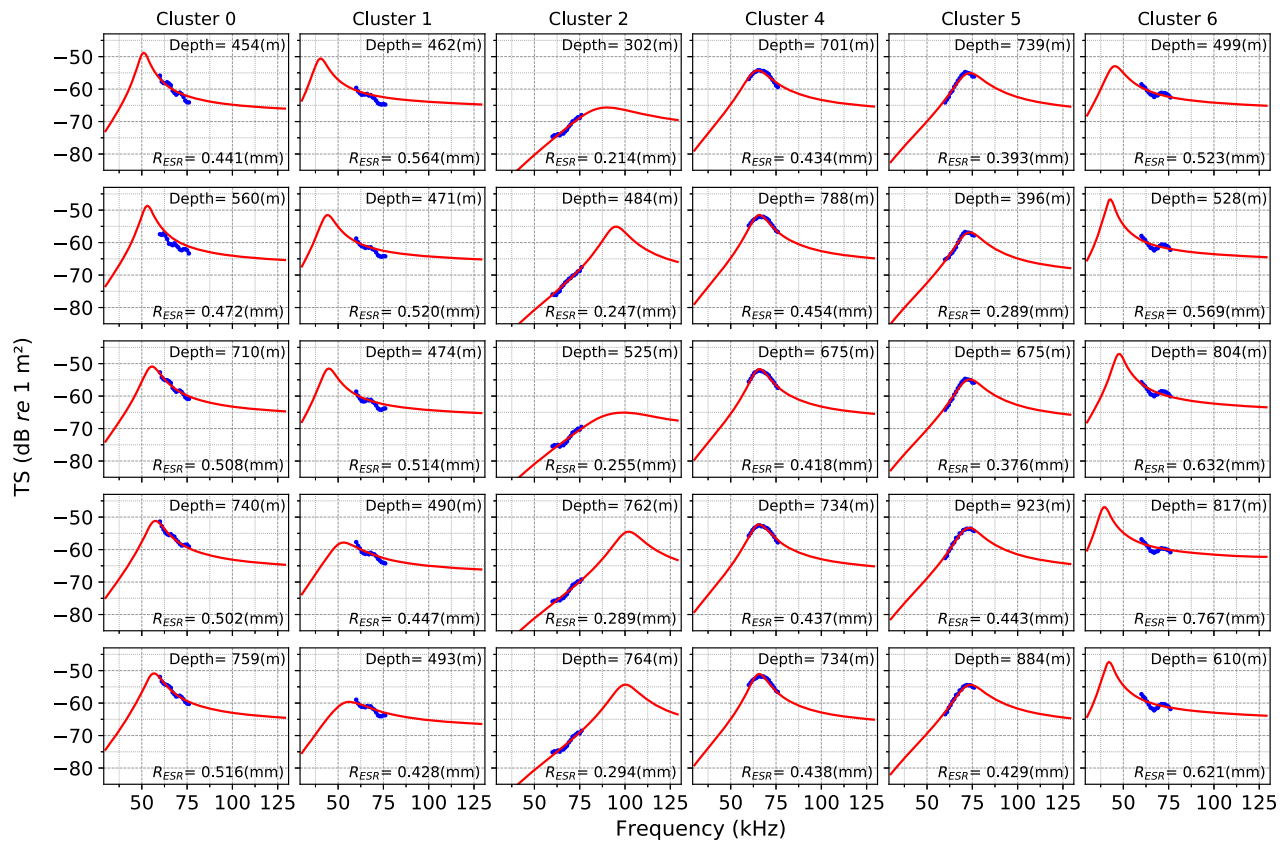


Figure 3. *In situ* measured TS ($\text{dB re } 1 \text{ m}^2$) as a function of frequency (kHz) (TS spectra, blue line) for randomly chosen single targets close to the centroids of each cluster type (five targets per cluster type) measured from 60 to 76 kHz. Model fitting (red line) of the viscous–elastic scattering model presented in Khodabandloo *et al.* (2021) to the measured TS spectra. The resulting ESR of the swimbladder (R_{ESR}), together with depth (m) of each target is stated. No C3 targets were situated close to the centroid. See Supplementary Figure S3 for *in situ* examples of wideband (38 + 55–237 kHz) single TS spectra.

groups *in situ* (e.g. Stanton *et al.*, 1996; Bassett *et al.*, 2020). Here, we demonstrate the utility of broadband acoustic data, in connection with an unsupervised clustering algorithm, in objectively describing and decomposing patterns of spatial structure and abundances of acoustic categories. Clustering algorithms objectively identify patterns in the data (e.g. Jain *et al.*, 1999), and various clustering analyses have previously been applied on different types of acoustic data (Peña, 2018; Proud *et al.*, 2018). AC separates targets based on patterns in their $r(f)$, which is clear when looking at the randomly chosen single targets in Figure 3. Some cluster types overlap in the PCA space, indicating similar $r(f)$ and resonance frequencies. The shape of $r(f)$ s were similar for C0, C1, and C6, but TS spectra slightly different (Figure 2). Yet, when comparing the model-fitted $r(f)$ s of the random targets of these cluster types, it is evident that the targets have overlapping swimbladder sizes and a wide range of resonance frequencies (<60 kHz) (Figure 3).

As a trade-off between time consumption and handling big data, target $r(f)$ s were generated from TS's automatically detected using a single echo detection algorithm (Ona, 1999) in the program LSSS. We reduced the probability of having more than one target in the acoustic beam by only including targets 9–12 m away from MESSOR. However, the deep null in the $r(f)$ of C3 targets might be an indication of that some targets could not be separated [see Figure 2 and Supplementary Figure S3d in current paper and e.g. Figure 2 in

Khodabandloo *et al.* (2021)]. A similar $r(f)$ was described as “complex” by Bassett *et al.* (2020) who also looked at $r(f)$ of mesopelagic fish from broadband acoustic measurements. C3 targets stood out in the AC results when plotted in PCA space, but only contributed 0.04% to the total number of targets in the mesopelagic zone.

We cannot exclude that larger swimbladdered fish, generally capable of higher swimming speeds than smaller fish (Bainbridge, 1958) and which would have lower resonance frequency, might have avoided MESSOR. The vertical distribution of backscatter at 18 kHz (observed from the hull-mounted acoustics) had peaks from 200 to 600 m depth in all regions, but these backscattering peaks were not observed in neither 38- nor 70 kHz hull-mounted, nor were these backscattering peaks at 18 kHz accompanied by peaks in organismal densities detected by MESSOR at 70 kHz. This high backscatter measured at 18 kHz could thus potentially be an indication of avoidance behaviour from organisms with resonance frequency close to 18 kHz and highlights the frequency-dependent nature of mesopelagic backscatter. This is further supported by observed DVM patterns at 18 kHz, even in the central region where MESSOR data indicates little DVM. Nonetheless, when comparing our *in situ* numerical density estimates with those estimated from trawl catch data, estimates obtained from echo-counting (current study) result in higher densities compared to those obtained from trawls [Supplementary Table S1 in García-Seoane *et al.* (2021)]. Net samples are though needed to get

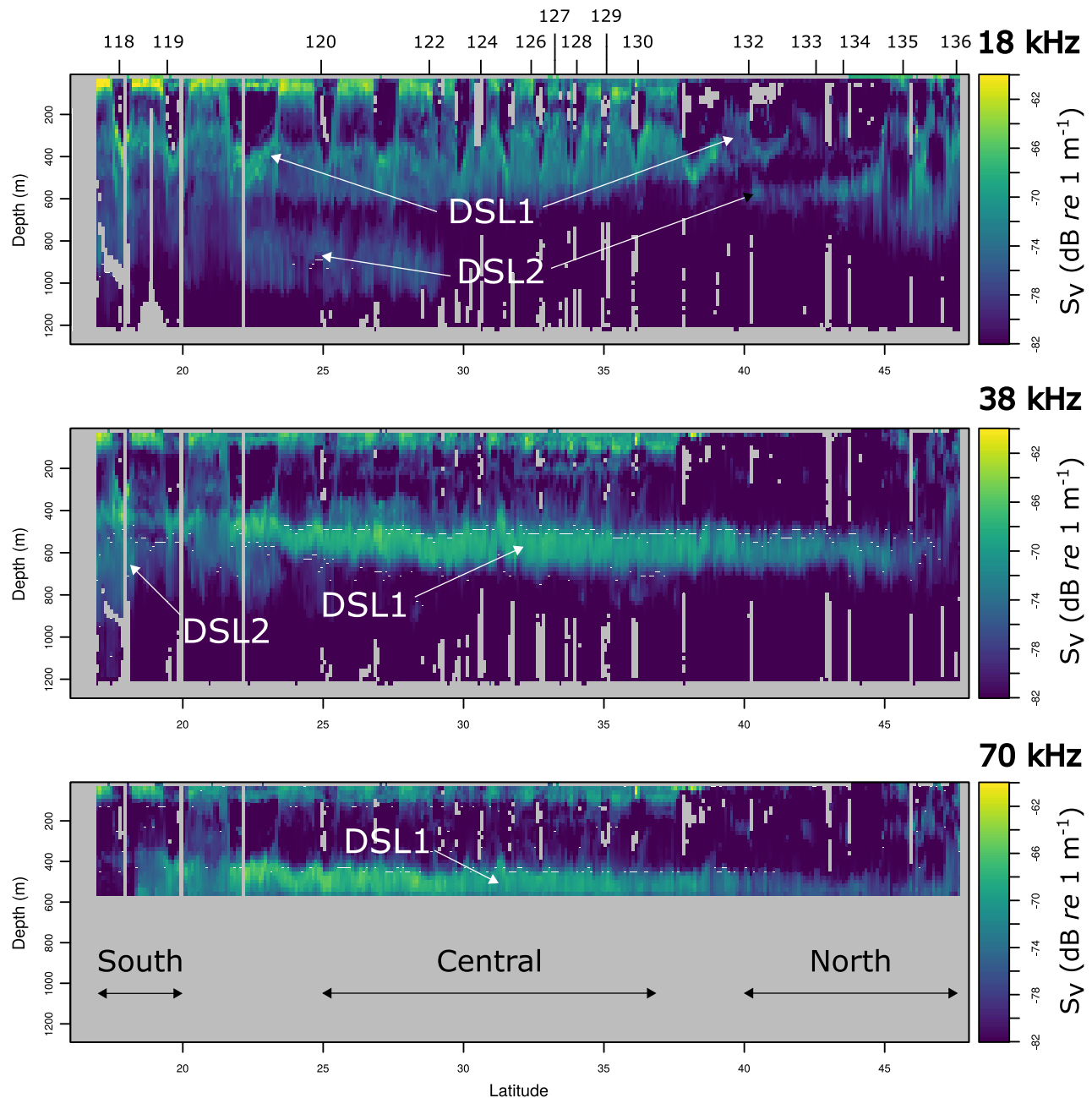


Figure 4. Echograms from hull-mounted acoustic measurements along the cruise track from south to north (Figure 1) showing backscattering strength (S_v , dB re 1 m^{-1}) both day and night at 18, 38, and 70 kHz (from top to bottom panel). Due to absorption, 70 kHz only reaches to ~ 560 m depth. DSLs in the mesopelagic zone are indicated as DSL1 (upper DSL) and DSL2 (deeper DSL). Station locations shown on top.

qualitative data for ground-truthing but indeed suffer from extrusion of smaller species through nets and potentially from avoidance by larger individuals (Kaartvedt *et al.*, 2012; Olivar *et al.*, 2017).

Abundance and biomass estimation of mesopelagic communities and the implication of resonance

Due to the ubiquity of 38 kHz transducers, as well as the capability of this frequency to cover the entire mesopelagic zone, many studies have used and continue to use hull-mounted 38 kHz data

to estimate abundance and biomass of mesopelagic fish (Irigoien *et al.*, 2014; Proud *et al.*, 2019; Haris *et al.*, 2021), as well as to describe vertical distribution and migration of mesopelagic organisms (e.g. Klevjer *et al.*, 2016, 2019). Previous studies have linked distribution patterns of mesopelagic organisms to biological and physical parameters based on acoustic data collected at 38 kHz (e.g. Klevjer *et al.*, 2016; Aksnes *et al.*, 2017). Although widely used in ecological studies, 38 kHz does not capture all macroplankton and micronekton components of the mesopelagic community equally [e.g. Figure 3 in Underwood *et al.* (2020)], thus likely missing

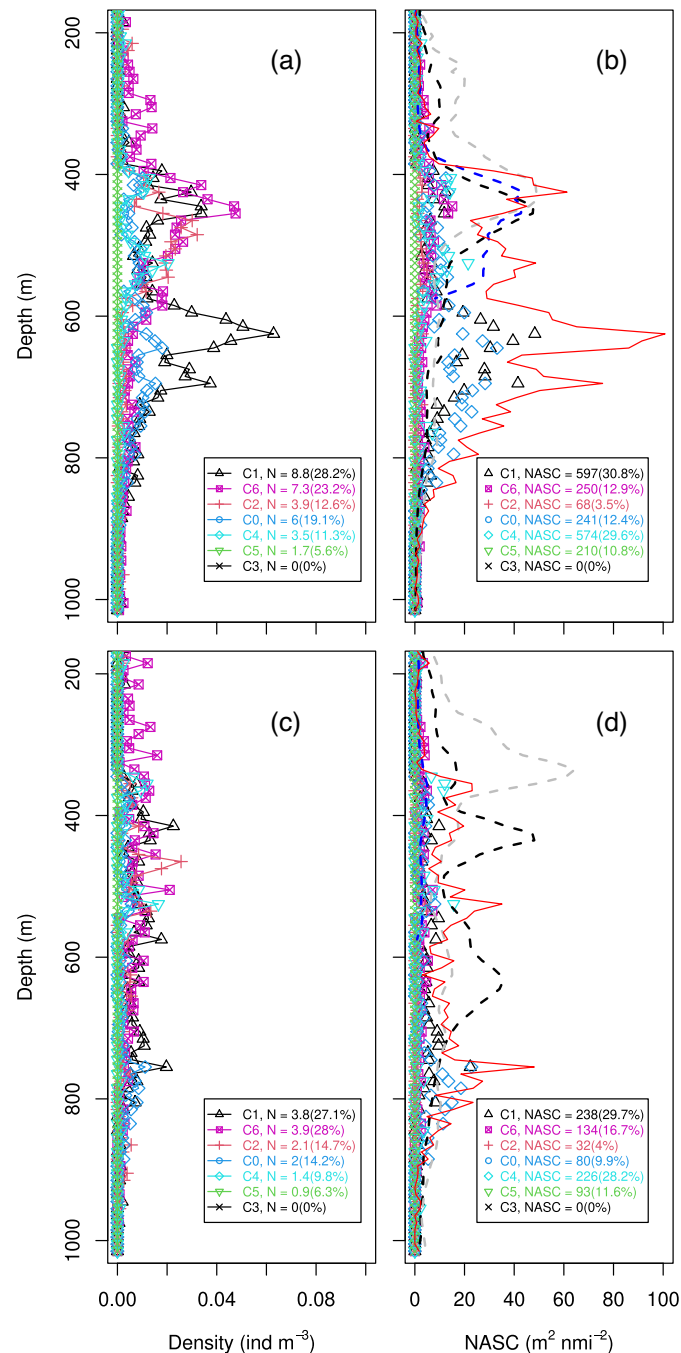


Figure 5. Density (ind. m⁻³) distributions of the seven cluster types based on echo-counts from MESSOR in the southern region during day (a) and night (c). (b) day- and (d) night-time backscatter (nautical area scattering coefficient; NASC, m² nmi⁻²) for the seven cluster types and hull-mounted data in the southern region. In (b) and (d), the black broken line shows vertical distribution of 38 kHz backscatter seen from the hull-mounted transducer, within an hour of the MESSOR deployment. The grey broken line is 18 kHz data, and the blue broken line 70 kHz data. NASC-values for the different cluster types are synthetic, i.e. estimated based on *in situ* densities (echo-counting) and TS measurements obtained from MESSOR data. The red line shows synthetic 70 kHz NASC estimates when all clusters are combined. Legends in (a) and (c) show the different clusters, their integrated abundances (200–1000 m; ind. m⁻³), and their relative importance (%). Legends in (b) and (d) show absolute and relative cluster contribution to total NASC in the depth range.

correlations between some mesopelagic organismal groups and the surrounding environment.

One issue in the current (and long-held) “mesopelagic acoustic paradigm” is that the use of data from hull-mounted 38 kHz

transducers for assessment of mesopelagic biomasses is problematic, due to resonance effects caused by both mesopelagic fish and siphonophores. Previous studies have tried to assess the implications of resonance effects on abundance and biomass estimates from

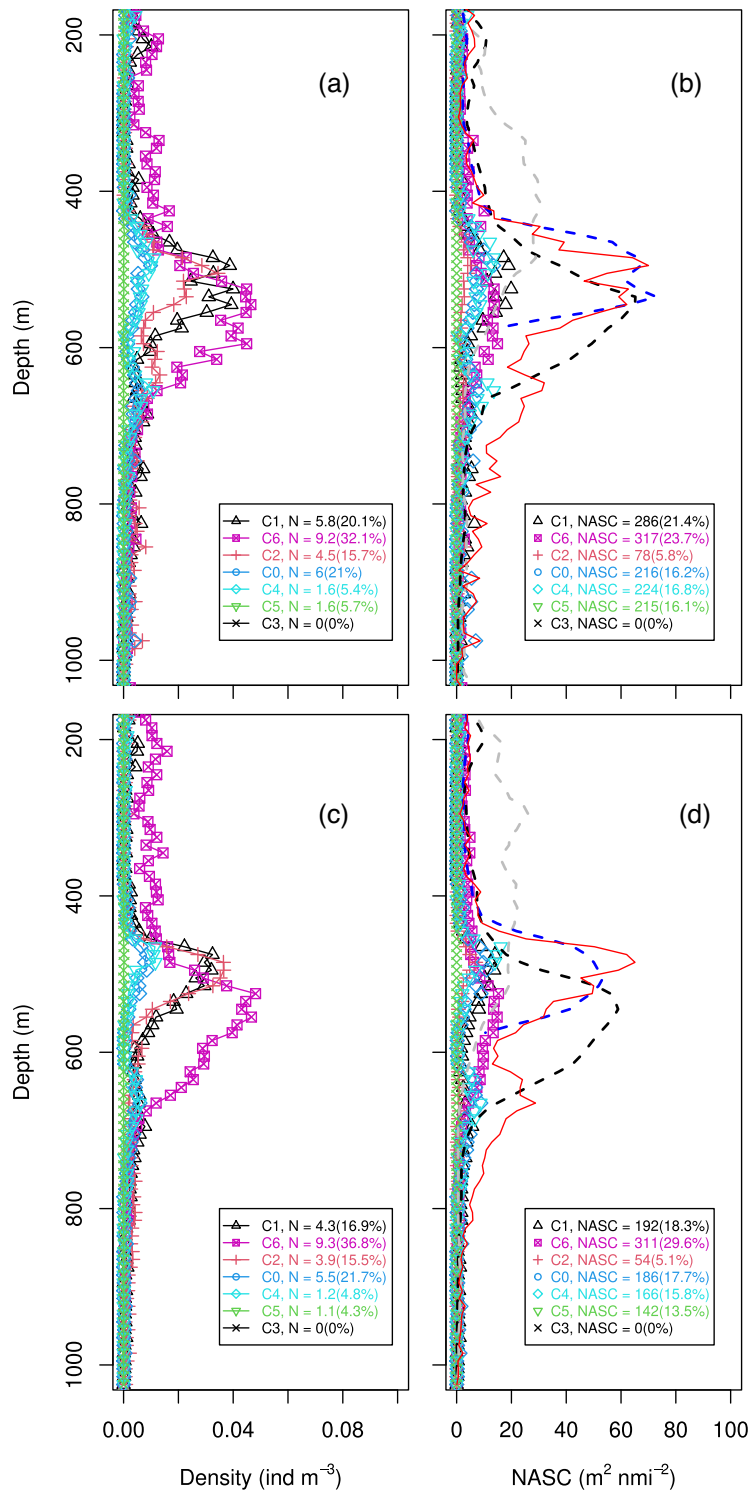


Figure 6. Density (ind. m⁻³) distributions of the seven cluster types based on echo-counts from MESSOR in the central region during day (a) and night (c). (b) day- and (d) night-time backscatter (NASC, m² nmi⁻²) for the seven cluster types and hull-mounted data in the central region. See Figure 5 for details.

38 kHz data by modelling TS distributions using size-distributions from either catches (e.g. Davison *et al.*, 2015) or modelling efforts (Proud *et al.*, 2019). Evaluating *in situ* densities of organisms, estimated by echo-counting, against results from hull-mounted data

(Kloser *et al.*, 2009; Kloser *et al.*, 2016; Cotter *et al.*, 2021b) is an alternative approach that, when combined with information on the frequency response of the organisms, can be used to assess the relative importance of resonance for mesopelagic biomass studies

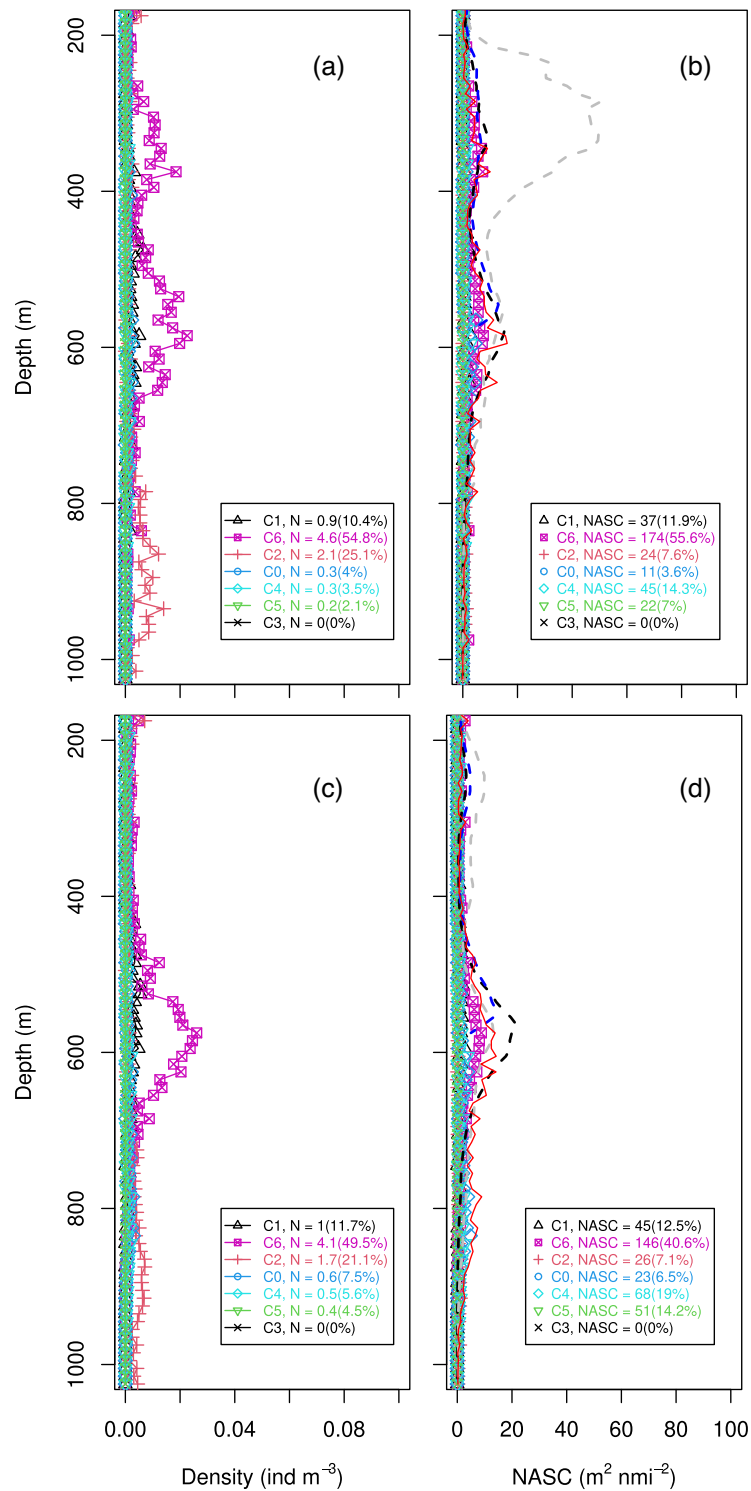


Figure 7. Density (ind. m⁻³) distributions of the seven cluster types based on echo-counts from MESSOR in the northern region during day (a) and night (c). (b) day- and (d) night-time backscatter (NASC, m² nmi⁻²) for the seven cluster types in the northern region. See Figure 5 for details.

(Kloser *et al.*, 2016). The advantage of this method is that targets are directly counted from acoustic measurements, and the frequency response of the target directly can indicate the resonant frequency of the air-inclusion, although that would require broadband acoustic measurements at lower frequencies than

applied in the current study. Echo-counting could though be prone to suffer from avoidance, since short ranges are needed in order to resolve individual targets. Yet, applying broadband acoustic data for echo-counting likely enables inclusion of targets further away than when narrowband data are applied due to the increased range

resolution (e.g. Stanton *et al.*, 2010). Abundance and biomass estimations depend on correct assumptions regarding backscattering properties of the different organismal groups, and that the general community composition is known. Mesopelagic scattering layers are likely comprised of a mix of different species and organismal groups (e.g. Ariza *et al.*, 2016; Figures 5–7 in the current study). As shown in the present study and by Bassett *et al.* (2020), a fraction of mesopelagic micronektonic targets may either have “resonant backscattering” peaking at higher frequencies, or not have air-inclusions. Both groups may have low TS at 38 kHz and they may therefore contribute very little to scattering at 38 kHz (Underwood *et al.*, 2020).

In field studies, one will always have to make a trade-off between sampling costs (in effort and money) and the quality of the data. The present results highlight two separate problems with using single frequency data to estimate mesopelagic biomass/abundance: one being the lack of knowledge on acoustic properties of mesopelagic organisms, the second being that the low frequency data (needed to penetrate the mesopelagic zone) will be better suited to observing a subset of the mesopelagic biomass, and is in practice likely to be dominated by those organisms with gas inclusions in the right size range. Studies from both the southern ocean (e.g. Dornan *et al.*, 2019; Escobar-Flores *et al.*, 2020) and the north Atlantic (Klevjer *et al.*, 2019) have described strong gradients in mesopelagic backscatter over areas with more or less constant levels of biomass of mesopelagic fish, highlighting the importance of gradients in scattering properties at higher latitudes. While the current state of knowledge about acoustic properties of mesopelagic organisms can be improved by more sampling and studies, ultimately allowing us to produce better estimates of TS for the organisms we observe with the acoustics, the “visibility bias” lead to overlooking targets that are weaker scatterers at lower frequencies and could potentially bias our understanding of global mesopelagic distribution patterns.

In a similar study from the western Atlantic, Cotter *et al.* (2021a) looked at broadband spectra (25–40 kHz) of mesopelagic organisms obtained from a towed acoustic platform and applied a physics-informed machine learning algorithm to group targets, and they point out that classification of a gas-bearing target or a fluid-filled organisms (in the latter’s geometric scattering regime), can be ambiguous. TS histograms from mesopelagic depths indicated a local numerical minimum close to a TS of -68 dB *re* 1 m² at 70 kHz, which we therefore applied as TS threshold to separate stronger (likely gas-bearing) from weaker (e.g. crustaceans) targets. We cannot exclude though, that some of the detected targets in the present study, e.g. cluster type 2 (C2; Figures 2 and 3), could be large fluid-filled targets such as non-swimbladdered fish [see e.g. Figure 2 in Davison (2011)].

Here, we only focused on stronger acoustic targets (i.e. organisms with a gas inclusion). Our acoustic data from MESSOR include backscatter measurements at higher frequencies (96–237 kHz) as well, which should be used in future studies to investigate spatial patterns of “broader” taxonomic functional groups like crustaceans and non-swimbladdered fish to improve our understanding of mesopelagic ecosystems.

Spatial distribution of mesopelagic gas-bearing organisms

Knowledge on vertical structures of mesopelagic organisms is limited but important for understanding functioning and roles of

mesopelagic ecosystems. From the analysed data, it is evident that the vertical distribution patterns of DSLs and the seven different target (cluster) types differ spatially and correlate with different biogeographic regions (Sutton *et al.*, 2017; García-Seoane *et al.*, 2021). Sutton *et al.* (2017) defined global ecoregions of the mesopelagic zone based on biodiversity and function. The south, central, and north defined in the present study based on acoustic measurement are situated within the ecoregions Mauritania/Cape Verde, Central North Atlantic, and North Atlantic drift, respectively (Sutton *et al.*, 2017). García-Seoane *et al.* (2021) used trawl data from the same cruise as in the present study, excluding southern stations (118 and 119). By multivariate analysis, they found that the mesopelagic fish species communities were divided into two clusters: 25–37°N (stations 122–130) and 42–48°N (stations 133–136), corresponding to the central and north regions, respectively, defined in the present study.

Integrated numerical densities of targets in the mesopelagic zone were similar in the south and central during daytime and approximately three times higher than those in the north. In the south, the density at night was half of what was estimated during day, indicating substantial DVM. The two DSLs in the southern region both occur within the oxygen minimum zone (OMZ; e.g. Karstensen *et al.*, 2008; García-Seoane *et al.*, 2021). The observed DVM supports that organisms living in OMZs would need to migrate to more oxygenated surface waters during night to replenish any deficit in oxygen, while at the same time being protected from visual predators [review by Seibel (2011) and references therein]. Moreover, the shallower distribution of DSL1 in the south fits with the hypothesis that diel vertical migrators can reduce their migration amplitude in low-oxygen areas, since larger visual predators tend to have higher oxygen requirements and therefore are excluded from the OMZ (e.g. Seibel, 2011; Bianchi *et al.*, 2013). In the central and northern regions, the density of targets in DSL1 was very similar day and night, indicating minimal, if any, DVM to and from the layer.

Our data indicate differences in numerical densities and vertical distributions of the different cluster types, which is especially evident in the central region where a permanent DSL is observed day and night. For example, peak densities of target types with resonance frequencies >60 kHz (C2 and C4–C5; Table 2 and Figure 3) occurred a bit shallower than C6 targets, which are likely larger targets with larger swimbladders and thus a lower resonance frequency. This observation is supported by previous studies that found a positive correlation between depth of occurrence and size of the fish (i.e. shallower occurrence of smaller fish and deeper occurrence of larger) (e.g. Badcock and Merrett, 1976; Olivar *et al.*, 2012). However, ontogenetic differences in swimbladder sizes have been observed in some mesopelagic fish species, where larger individuals have fat-invested swimbladders and therefore smaller swimbladders than smaller individuals (e.g. Marshall, 1960; Davison, 2011), thus complicating interpretation of the acoustic data. Mapping of the acoustic categories to taxonomic groups is further complicated by lack of knowledge about swimbladder responses to changes in depth: do the fish maintain close to neutral buoyancy (i.e. swimbladder size is constant with depth) during the DVM? This would affect the resonant frequency for a given fish at a given depth, which already is pressure dependent. The clusters therefore represent organisms with similar acoustic properties, rather than taxonomic or size groupings. With that in mind, a given organism is more likely to have similar acoustic properties with a conspecific of the same size than with an organism of different taxonomy and size.

The resulting frequency responses were within the TS range expected from organisms with a gas inclusion, including both swimbladder fish and physonect siphonophores (e.g. Kloser *et al.*, 2016; Proud *et al.*, 2019; Bassett *et al.*, 2020). We did not have dedicated sampling for siphonophores on the cruise. However, nets [Multinet MAMMOTH and a macroplankton trawl with mesh opening of 3 mm × 3 mm (8 mm stretched; non-graded)] were never fouled with siphonophore remnants as has been observed in instances where siphonophores dominated the acoustic backscatter (Knutsen *et al.*, 2018), which suggests relatively low densities of these organisms in the area. Therefore, we assume targets observed in the acoustic data are mainly swimbladder fish and not siphonophores. The estimated swimbladder sizes (Figure 3) were additionally within the range of previously reported values for mesopelagic swimbladder fish (e.g. Marshall, 1960; Saenger, 1989; Davison, 2011). There is a high possibility that the targets that were measured 9–12 m from MESSOR were dominated by smaller fish targets, as many mesopelagic fish species can avoid gear (Koslow *et al.*, 1995; Kaartvedt *et al.*, 2012). Trawl catches from the same area, presented in García-Seoane *et al.* (2021), indicated that four species of *Cyclothone* (family: Gonostomatidae) constituted more than 78% of the total fish density in the studied area, though likely underestimated due to extrusion through meshes because of their small size and slender shape (Oliver *et al.*, 2012, 2017). Species of *Cyclothone* likely do not have significant avoidance behaviour (Peña *et al.*, 2020) and similar could be the case for smaller individuals of other species.

Conclusions

Our findings of target type categories indicate that likely more than 30% of the acoustically identified targets had resonance frequencies >38 kHz and low TSs at this normally applied frequency for density estimates of mesopelagic fish. Studies relying solely on 38 kHz data therefore run the risk of underestimating the abundance of these organisms. Our results further suggest that towed acoustic platforms are a great supplement to hull-mounted acoustics, both for direct density estimates via echo-counting and for obtaining TSs for different target groups at different frequencies, also at depths where higher acoustic frequencies cannot reach if transmitted from the surface. While hull-mounted acoustic data can visualize the whole water column and cover large areas, towed platforms can provide fine-scale measurements of distribution patterns of mesopelagic communities, though at limited spatial coverage. As organismal assemblages are rarely uniform but consist of a mix of species and organismal groups, data from towed acoustic platforms could furthermore support catch data obtained from nets, which often sample through large vertical depth strata, thus complicating identification of the depth of residence of organisms. Similar analyses as conducted here should be applied on acoustic data measured at lower and higher frequencies to investigate ecology of other mesopelagic organismal groups. If towed instrumented platforms are to be used in the future as an addition to hull-mounted acoustic systems, avoidance of mesopelagic organisms to the platforms should be investigated further.

Data availability

The data underlying this article will be shared on reasonable request to the corresponding author.

Supplementary Data

Supplementary material is available at the ICESJMS online version of the manuscript.

Funding

Funding for this work was provided by the HARMES project, the Research Council of Norway (project number 280 546), and MEESO, EU H2020 research and innovation programme (grant agreement no. 817669).

Acknowledgement

We are grateful to the officers and crew onboard R/V Kronprins Haakon for any help provided.

References

- Aksnes, D. L., Røstad, A., Kaartvedt, S., Martinez, U., Duarte, C. M., and Irigoien, X. 2017. Light penetration structures the deep acoustic scattering layers in the global ocean. *Science Advances*, 3: e1602468.
- Andreeva, I. B., Galybin, N. N., and Tarasov, L. L. 2000. Vertical structure of the acoustic characteristics of deep scattering layers in the ocean. *Acoustical Physics*, 46: 505–510.
- Ariza, A., Landeira, J. M., Escáñez, A., Wienerroither, R., Aguilar de Soto, N., Røstad, A., Kaartvedt, S. *et al.* 2016. Vertical distribution, composition and migratory patterns of acoustic scattering layers in the Canary Islands. *Journal of Marine Systems*, 157: 82–91.
- Badcock, J., and Merrett, N. R. 1976. Midwater fishes in the eastern North Atlantic—I. Vertical distribution and associated biology in 30°N, 23°W, with developmental notes on certain myctophids. *Progress in Oceanography*, 7: 3–58.
- Bainbridge, R. 1958. The speed of swimming of fish as related to size and to the frequency and amplitude of the tail beat. *Journal of Experimental Biology*, 35: 109–133.
- Bassett, C., De Robertis, A., Wilson, C. D., and Ratilal, H. e. P. 2018. Broadband echosounder measurements of the frequency response of fishes and euphausiids in the Gulf of Alaska. *ICES Journal of Marine Science*, 75: 1131–1142.
- Bassett, C., Lavery, A. C., Stanton, T. K., and Cotter, E. D. 2020. Frequency- and depth-dependent target strength measurements of individual mesopelagic scatterers. *The Journal of the Acoustical Society of America*, 148: EL153–EL158.
- Bernardes, I. D., Ona, E., and Gjøsæter, H. 2020. Study of the Arctic mesopelagic layer with vessel and profiling multifrequency acoustics. *Progress in Oceanography*, 182: 102260.
- Bianchi, D., Galbraith, E. D., Carozza, D. A., Mislán, K. A. S., and Stock, C. A. 2013. Intensification of open-ocean oxygen depletion by vertically migrating animals. *Nature Geoscience*, 6: 545–548.
- Cotter, E., Bassett, C., and Lavery, A. 2021. Classification of broadband target spectra in the mesopelagic using physics-informed machine learning. *The Journal of the Acoustical Society of America*, 149: 3889–3901.
- Cotter, E., Bassett, C., and Lavery, A. 2021. Comparison of mesopelagic organism abundance estimates using *in situ* target strength measurements and echo-counting techniques. *JASA Express Letters*, 1: 040801.
- Davison, P. 2011. The specific gravity of mesopelagic fish from the northeastern Pacific Ocean and its implications for acoustic backscatter. *ICES Journal of Marine Science*, 68: 2064–2074.
- Davison, P. C., Checkley, D. M. Jr, Koslow, J. A., and Barlow, J. 2013. Carbon export mediated by mesopelagic fishes in the northeast Pacific Ocean. *Progress in Oceanography*, 116: 14–30.
- Davison, P. C., Koslow, J. A., and Kloser, R. J. 2015. Acoustic biomass estimation of mesopelagic fish: backscattering from individuals, populations, and communities. *ICES Journal of Marine Science*, 72: 1413–1424.

- De Robertis, A., McKelvey, D. R., and Ressler, P. H. 2010. Development and application of an empirical multifrequency method for backscatter classification. *Canadian Journal of Fisheries and Aquatic Sciences*, 67: 1459–1474.
- Demer, D. A., Berger, L., Bernasconi, M., Bethke, E., Boswell, K., Chu, D., Domokos, R. *et al.* 2015. Calibration of acoustic instruments. ICES Cooperative Research Report No. 326. 133 pp.
- Dornan, T., Fielding, S., Saunders, R. A., and Genner, M. J. 2019. Swimbladder morphology masks Southern Ocean mesopelagic fish biomass. *Proceedings of the Royal Society B: Biological Sciences*, 286: 20190353.
- Dypvik, E., Klevjer, T. A., and Kaartvedt, S. 2012. Inverse vertical migration and feeding in glacier lanternfish (*Benthoosema glaciale*). *Marine Biology*, 159: 443–453.
- Escobar-Flores, P. C., O'Driscoll, R. L., Montgomery, J. C., Ladroit, Y., and Jendersie, S. 2020. Estimates of density of mesopelagic fish in the Southern Ocean derived from bulk acoustic data collected by ships of opportunity. *Polar Biology*, 43: 43–61.
- Faran, J. J. Jr 1951. Sound scattering by solid cylinders and spheres. *The Journal of the Acoustical Society of America*, 23: 405–418.
- Feuillade, C., and Nero, R. 1998. A viscous-elastic swimbladder model for describing enhanced-frequency resonance scattering from fish. *The Journal of the Acoustical Society of America*, 103: 3245–3255.
- Foote, K. G. 1980. Importance of the swimbladder in acoustic scattering by fish: a comparison of gadoid and mackerel target strengths. *The Journal of the Acoustical Society of America*, 67: 2084–2089.
- Francois, R., and Garrison, G. 1982. Sound absorption based on ocean measurements. Part II: boric acid contribution and equation for total absorption. *The Journal of the Acoustical Society of America*, 72: 1879–1890.
- Francois, R., and Garrison, G. 1982. Sound absorption based on ocean measurements: part I: pure water and magnesium sulfate contributions. *The Journal of the Acoustical Society of America*, 72: 896–907.
- Furusawa, M. 2015. Effects of noise and absorption on high frequency measurements of acoustic-backscatter from fish. *International Journal of Oceanography*, 2015: 1.
- García-Seoane, E., Wienerroither, R., Mork, K. A., Underwood, M., and Melle, W. 2021. Biogeographical patterns of meso- and bathypelagic fish along a Northeastern Atlantic transect. *ICES Journal of Marine Science*, 78: 1444–1457.
- Gjosæter, J., and Kawaguchi, K. 1980. A review of the world resources of mesopelagic fish. *Fao Fish Technical Papers*, 193: 1–153.
- Haris, K., Kloser, R. J., Ryan, T. E., Downie, R. A., Keith, G., and Nau, A. W. 2021. Sounding out life in the deep using acoustic data from ships of opportunity. *Scientific Data*, 8: 1–23.
- Hays, G. C. 2003. A review of the adaptive significance and ecosystem consequences of zooplankton diel vertical migrations. *Hydrobiologia*, 503: 163–170.
- Hickling, R. 1962. Analysis of echoes from a solid elastic sphere in water. *The Journal of the Acoustical Society of America*, 34: 1582–1592.
- Horne, J. K. 2000. Acoustic approaches to remote species identification: a review. *Fisheries Oceanography*, 9: 356–371.
- Irigoin, X., Klevjer, T. A., Røstad, A., Martinez, U., Boyra, G., Acuña, J. L., Bode, A. *et al.* 2014. Large mesopelagic fishes biomass and trophic efficiency in the open ocean. *Nature communications*, 5: 3271.
- Jain, A. K., Murty, M. N., and Flynn, P. J. 1999. Data clustering: a review. *ACM Computing Surveys*, 31: 264–323.
- Javed, M. A., Younis, M. S., Latif, S., Qadir, J., and Baig, A. 2018. Community detection in networks: a multidisciplinary review. *Journal of Network and Computer Applications*, 108: 87–111.
- Kaartvedt, S., Staby, A., and Aksnes, D. L. 2012. Efficient trawl avoidance by mesopelagic fishes causes large underestimation of their biomass. *Marine Ecology Progress Series*, 456: 1–6.
- Karstensen, J., Stramma, L., and Visbeck, M. 2008. Oxygen minimum zones in the eastern tropical Atlantic and Pacific oceans. *Progress in Oceanography*, 77: 331–350.
- Kelley, D. E., and Richards, C. 2020. oce: Analysis of Oceanographic Data. R package version 1.2-0. <https://CRAN.R-project.org/package=oce> (accessed 28 March 2021).
- Khodabandello, B., Agersted, M. D., Klevjer, T. A., Macaulay, G. J., and Melle, W. 2021. Estimating target strength and physical characteristics of gas-bearing mesopelagic fish from wideband *in situ* echoes using a viscous-elastic scattering model. *The Journal of the Acoustical Society of America*, 149: 673–691.
- Klevjer, T., Melle, W., Knutsen, T., Strand, E., Korneliussen, R., Dupont, N., Salvanes, A. G. V. *et al.* 2019. Micronekton biomass distribution, improved estimates across four north Atlantic basins. *Deep Sea Research Part II: Topical Studies in Oceanography*, 180: 104691.
- Klevjer, T. A., Irigoien, X., Røstad, A., Fraile-Nuez, E., Benítez-Barrios, V. M., and Kaartvedt, S. 2016. Large scale patterns in vertical distribution and behaviour of mesopelagic scattering layers. *Scientific Reports*, 6: 19873.
- Klevjer, T. A., Torres, D. J., and Kaartvedt, S. 2012. Distribution and diel vertical movements of mesopelagic scattering layers in the Red Sea. *Marine Biology*, 159: 1833–1841.
- Kloser, R. J., Ryan, T. E., Keith, G., and Gershwin, L. 2016. Deep-scattering layer, gas-bladder density, and size estimates using a two-frequency acoustic and optical probe. *ICES Journal of Marine Science*, 73: 2037–2048.
- Kloser, R. J., Ryan, T. E., Young, J. W., and Lewis, M. E. 2009. Acoustic observations of micronekton fish on the scale of an ocean basin: potential and challenges. *ICES Journal of Marine Science*, 66: 998–1006.
- Knutsen, T., Hosaia, A., Falkenhaus, T., Skern-Mauritzen, R., Wiebe, P., Larsen, R. B., Aglen, A. *et al.* 2018. Coincident mass occurrence of gelatinous zooplankton in northern Norway. *Frontiers in Marine Science*, 5: 158, doi: 10.3389/fmars.2018.00158.
- Knutsen, T., Melle, W., Mjanger, M., Strand, E., Fuglestad, A.-L., Broms, C., Bagoien, E. *et al.* 2013. MESSOR - a towed underwater vehicle for quantifying and describing the distribution of pelagic organisms and their physical environment. 2013 MTS/IEEE OCEANS-Bergen. 1–12pp.
- Korneliussen, R. J., Heggelund, Y., Macaulay, G. J., Patel, D., Johnsen, E., and Eliassen, I. K. 2016. Acoustic identification of marine species using a feature library. *Methods in Oceanography*, 17: 187–205.
- Korneliussen, R. J., and Ona, E. 2002. An operational system for processing and visualizing multi-frequency acoustic data. *ICES Journal of Marine Science*, 59: 293–313.
- Koslow, J. A., Kloser, R., and Stanley, C. A. 1995. Avoidance of a camera system by a deepwater fish, the orange roughy (*Hoplostethus atlanticus*). *Deep Sea Research Part I: Oceanographic Research Papers*, 42: 233–244.
- Lavery, A. C., Chu, D., and Moum, J. N. 2010. Measurements of acoustic scattering from zooplankton and oceanic microstructure using a broadband echosounder. *ICES Journal of Marine Science*, 67: 379–394.
- Marshall, N. B. 1960. Swimbladder Structure of Deep-sea Fishes in Relation to Their Systematics and Biology *Discovery Reports*, 31: 1–121.
- Mulligan, T. 2000. Shallow water fisheries sonar: a personal view. *Aquatic Living Resources*, 13: 269–273.
- Olivar, M. P., Bernal, A., Molí, B., Peña, M., Balbín, R., Castellón, A., Miquel, J. *et al.* 2012. Vertical distribution, diversity and assemblages of mesopelagic fishes in the western Mediterranean. *Deep Sea Research Part I: Oceanographic Research Papers*, 62: 53–69.
- Olivar, M. P., Hulley, P. A., Castellón, A., Emelianov, M., López, C., Tuset, V. M., Contreras, T. *et al.* 2017. Mesopelagic fishes across the tropical and equatorial Atlantic: biogeographical and vertical patterns. *Progress in Oceanography*, 151: 116–137.
- Ona, E. 1999. Methodology for target strength measurements. *ICES Cooperative Research Report*, 235: 59.
- Peña, M. 2018. Robust clustering methodology for multi-frequency acoustic data: a review of standardization, initialization and cluster geometry. *Fisheries Research*, 200: 49–60.

- Peña, M., Cabrera-Gómez, J., and Domínguez-Brito, A. C. 2020. Multi-frequency and light-avoiding characteristics of deep acoustic layers in the North Atlantic. *Marine Environmental Research*, 154: 104842.
- Proud, R., Cox, M. J., Le Guen, C., and Brierley, A. S. 2018. Fine-scale depth structure of pelagic communities throughout the global ocean based on acoustic sound scattering layers. *Marine Ecology Progress Series*, 598: 35–48.
- Proud, R., Handegard, N. O., Kloser, R. J., Cox, M. J., and Brierley, A. S. 2019. From siphonophores to deep scattering layers: uncertainty ranges for the estimation of global mesopelagic fish biomass. *ICES Journal of Marine Science*, 76(3): 718–733.
- R Core Team 2018. R: A Language and Environment for Statistical Computing. R Foundation for Statistical Computing, Vienna, Austria.
- Robinson, C., Steinberg, D. K., Anderson, T. R., Arístegui, J., Carlson, C. A., Frost, J. R., Ghiglione, J.-F. *et al.* 2010. Mesopelagic zone ecology and biogeochemistry – a synthesis. *Deep Sea Research Part II: Topical Studies in Oceanography*, 57: 1504–1518.
- Saenger, R. A. 1989. Bivariate normal swimbladder size allometry models and allometric exponents for 38 mesopelagic swimbladdered fish species commonly found in the North Sargasso Sea. *Canadian Journal of Fisheries and Aquatic Sciences*, 46: 1986–2002.
- Seibel, B. A. 2011. Critical oxygen levels and metabolic suppression in oceanic oxygen minimum zones. *Journal of Experimental Biology*, 214: 326–336.
- Simmonds, J., and MacLennan, D. N. 2005. *Fisheries Acoustics: Theory and Practice*. Blackwell Science, Oxford, UK.
- Stanton, T. K., Chu, D., Jech, J. M., and Irish, J. D. 2010. New broadband methods for resonance classification and high-resolution imagery of fish with swimbladders using a modified commercial broadband echosounder. *ICES Journal of Marine Science*, 67: 365–378.
- Stanton, T. K., Chu, D., and Wiebe, P. H. 1996. Acoustic scattering characteristics of several zooplankton groups. *ICES Journal of Marine Science*, 53: 289–295.
- Stanton, T. K., Wiebe, P. H., and Chu, D. 1998. Differences between sound scattering by weakly scattering spheres and finite-length cylinders with applications to sound scattering by zooplankton. *The Journal of the Acoustical Society of America*, 103: 254–264.
- Subramaniyan, M., Skoogh, A., Muhammad, A. S., Bokrantz, J., Johansson, B., and Roser, C. 2020. A generic hierarchical clustering approach for detecting bottlenecks in manufacturing. *Journal of Manufacturing Systems*, 55: 143–158.
- Sutton, T. T., Clark, M. R., Dunn, D. C., Halpin, P. N., Rogers, A. D., Guinotte, J., Bograd, S. J. *et al.* 2017. A global biogeographic classification of the mesopelagic zone. *Deep Sea Research Part I: Oceanographic Research Papers*, 126: 85–102.
- Underwood, M. J., García-Seoane, E., Klevjer, T. A., Macaulay, G. J., and Melle, W. 2020. An acoustic method to observe the distribution and behaviour of mesopelagic organisms in front of a trawl. *Deep Sea Research Part II: Topical Studies in Oceanography*, 180: 104873.
- Ward, J. H. 1963. Hierarchical grouping to optimize an objective function. *Journal of the American Statistical Association*, 58: 236–244.
- Ye, Z., and Hoskinson, E. 1998. Low-frequency acoustic scattering by gas-filled prolate spheroids in liquids. II. Comparison with the exact solution. *The Journal of the Acoustical Society of America*, 103: 822–826.

Handling Editor: Roland Proud